Research Square

Preprints are preliminary reports that have not undergone peer review.
They should not be considered conclusive, used to inform clinical practice,
or referenced by the media as validated information.

Design and Simulation of CMUT Based on Graphene/Parylene-C Composite Membrane

Huan Li

3389146425@qq.com

southwest jiaotong university

YouMing Luo

southwest jiaotong university

YuCan Lei

southwest jiaotong university

Hai Han

southwest jiaotong university

YongLiang Chen

southwest jiaotong university

QuanFang Chen

southwest jiaotong university

Research Article

Keywords: Capacitive micromachined ultrasonic transducer (CMUT), Graphene-based composite membrane, ultrasonic phased array, COMSOL Multiphysics, medical imaging

Posted Date: November 11th, 2026

DOI: https://doi.org/10.21203/rs.3.rs-11497194/v1

License: This work is licensed under a Creative Commons Attribution 4.0 International License.
Read Full License

Additional Declarations: No competing interests reported.

Design and Simulation of CMUT Based on Graphene/Parylene-C Composite Membrane

Huan Li [a,b], Youming Luo [a], Yucan Lei [a], Hai Han [a,b], Yongliang Chen [a,*], Quanfang Chen [c,]**

[a] School of Electrical Engineering, Southwest Jiaotong University, Chengdu, 610031, China

[b] School of Physical Science and Technology, Southwest Jiaotong University, Chengdu, 610031, China

[c] School of Materials Science and Engineering, South China University of Technology, Guangzhou, 510640, China

**Corresponding authors, **Corresponding authors:*

llchen@home.swjtu.edu.cn (Yongliang Chen)

gaoshan2088@163.com (Quanfang Chen)

3389146425@qq.com (Huan Li)

Abstract：This paper proposes a capacitive micromachined ultrasonic transducer (CMUT) cell with a graphene/Parylene-C composite membrane, which takes full advantage of the excellent mechanical flexibility, low mass density and favorable electrical properties of the composite material to improve the electromechanical coupling efficiency and overall output performance of the ultrasonic transducer. A multi-physics finite-element model is established, and systematic parametric sweeps are carried out to investigate how key structural parameters including cavity radius, cavity height and membrane thickness influence the resonant frequency and dynamic vibration characteristics of the CMUT cell. According to the simulated results, optimal structural parameters are determined for the unit cell. On this basis, a CMUT phased array is designed targeting the operating resonant frequency of the optimized cell, and its acoustic directivity as well as beam-focusing performance are assessed via acoustic field numerical simulations. The simulation demonstrates that the developed composite-membrane CMUT phased array exhibits promising application potential for medical focused ultrasound imaging, and lays a simulation-driven foundation for the subsequent design and practical development of CMUT devices.

Keywords: Capacitive micromachined ultrasonic transducer (CMUT), Graphene-based composite membrane, ultrasonic phased array, COMSOL Multiphysics, medical imaging.

1 Introduction

Ultrasonic imaging is widely used in medical diagnosis and nondestructive testing because of its noninvasive nature, real-time capability, and relatively low cost. As a core component of an ultrasonic imaging system, the transducer plays a critical role in determining image quality and detection performance (Kobayashi et al. 2006; Guo et al. 2018; Li et al. 2022). Conventional ultrasonic transducers typically rely on piezoelectric ceramics, such as lead zirconate titanate (PZT). Although this technology is well established, it faces limitations in bandwidth, spatial resolution, and array integration (Boujenoui et al. 2025; Yu et al. 2026). Capacitive micromachined ultrasonic transducers (CMUTs), developed using microelectromechanical systems (MEMS) technology, offer an alternative to conventional piezoelectric transducers. Their advantages include broad fractional bandwidth, compatibility with densely integrated arrays, and the potential for direct integration with electronic circuits. These features make CMUTs promising candidates for real-time three-

dimensional ultrasonic imaging, portable medical diagnostic systems, and air-coupled ultrasonic nondestructive testing (Kashani et al. 2022).

Conventional CMUTs commonly use silicon or silicon nitride as vibrating membranes, benefiting from mature semiconductor microfabrication processes that enable precise structural control (Herickhoff et al. 2023). However, their acoustic performance remains subject to material and fabrication constraints. Silicon-based CMUTs typically have submicrometer cavity gaps, which limit the available membrane displacement and can constrain acoustic output. Insufficient acoustic output can, in turn, reduce the signal-to-noise ratio, imaging depth, and image quality (Adelegan et al. 2020). To overcome these limitations, researchers have increasingly explored flexible polymers and polymer composites as alternative membrane materials. For example, SU-8 (Chang et al. 2006)and polydimethylsiloxane (PDMS) (Chong et al. 2013) have been investigated for vibrating membranes. These approaches seek to exploit polymer flexibility and processing versatility to enable larger cavity gaps and improve acoustic output.

Parylene-C is a promising material for flexible CMUTs because of its mechanical toughness, biocompatibility, chemical stability, and ability to form thin, conformal films. It has been widely used for cavity sealing, surface passivation, and waterproof encapsulation in CMUT devices (He et al. 2021). However, Parylene-C is electrically insulating and therefore requires a conductive layer to enable electrostatic actuation in a composite membrane. Previous studies have demonstrated that combining Parylene-C with carbon-based nanomaterials can improve the electrical and mechanical properties of the resulting membrane. Liu et al. fabricated CMUTs incorporating single-walled carbon nanotube (SWCNT)/Parylene-C composite membranes with a Young's modulus of 4.4 GPa and a sheet resistance as low as 29.6 Ω/sq. The devices exhibited a resonant frequency of 2.108 MHz and a quality factor of 52.6 (Liu et al. 2023). These findings demonstrate the feasibility of carbon-based nanomaterial/polymer composite membranes and provide a foundation for further CMUT development.

Graphene is particularly attractive as a conductive reinforcement for CMUT membranes because of its high mechanical strength, excellent in-plane electrical conductivity, and atomically thin structure. Since its isolation in 2004, graphene has been extensively investigated for improving the performance of micro- and nanoscale sensors (Ma et al. 2012; Wan et al. 2026). incorporated graphene membranes into CMUTs and reported devices with a resonant frequency of 95 MHz (Chong et al. 2014). Combining graphene with Parylene-C offers a promising approach to providing electrical conductivity while addressing the adhesion and flexibility challenges associated with conventional metal electrodes. Graphene can also reinforce the membrane, while Parylene-C contributes flexibility and biocompatibility. These complementary properties offer the potential to improve the electromechanical performance and operational reliability of polymer-based CMUTs (Kim et al. 2017; Tavakoli et al. 2020).

Although simulations of individual CMUT cells can establish their resonant frequencies and vibration characteristics, cell-level analysis alone is insufficient to assess performance for imaging applications. A single cell can transmit and receive ultrasonic signals but cannot independently provide the electronically controlled focusing, beam steering, and scanning capabilities of a phased array. Ultrasonic phased arrays achieve focusing and steering by precisely controlling the relative excitation delays of their elements, thereby improving detection resolution and sensitivity(Xu et al. 2025). Evaluating CMUTs for imaging applications therefore requires both cell-level optimization

and array-level acoustic field analysis.

To address these challenges, this study proposes a graphene/Parylene-C composite membrane as the vibrating membrane of CMUTs, combining the complementary properties of the two materials to balance flexibility, mechanical stability, and electromechanical performance. A finite-element model coupling electrostatic, structural, and acoustic physics is developed in COMSOL Multiphysics. Parametric sweeps are conducted to systematically evaluate the effects of cavity radius, cavity height, and composite membrane thickness on the resonant frequency and vibration characteristics of the CMUT cell, enabling the identification of optimized structural parameters and the corresponding operating frequency. A one-dimensional CMUT phased array is then modeled using the optimized cell design. Acoustic field simulations are performed to assess the array's beam-focusing capability and lateral resolution. By integrating cell-level optimization, array modeling, and acoustic performance evaluation, this study assesses the potential of graphene/Parylene-C composite-membrane CMUTs for ultrasonic imaging and provides a simulation-based foundation for the design and optimization of flexible, high-performance CMUT phased arrays.

2 Theoretical and simulation

2.1 Vibration of Graphene/Parylene-C Composite Membrane

According to the definition in MEMS, when the width-to-thickness ratio exceeds 80:1, the thin-film vibration theory rather than the thin-plate vibration theory should be adopted to analyze CMUTs. The fundamental frequency of the bilayer composite membrane is (Liu et al. 2024):

$$f_{01} = \frac{2.405}{2\pi \mathrm{a}} \sqrt{\frac{T_1 + T_2}{h_1\rho_1 + h_2\rho_2}} \tag{1}$$

where a is the radius of the circular membrane, T_1 and T_2 are the tensions of the two membrane layers; h_1, h_2 and ρ_1, ρ_2 denote the thicknesses and tensions of the two membrane layers, respectively.

The tensions of the graphene layer and the Parylene-C layer can be expressed as:

$$T_g = E_g \dot{o}_g h_g \tag{2}$$

$$T_p = E_P \dot{o}_P h_P \tag{3}$$

In Equations (2) and (3), E_g and E_P represent the Young's moduli of graphene and Parylene-C, respectively; $\dot{o}_g$ and $\dot{o}_P$ are the strains under tension; h_g and h_P denote the thickness of each layer. The thickness of the graphene layer h_g can be further expressed as: Nh_{SLG}, where N is the number of graphene layers, and h_{SLG} is the thickness of a single-layer graphene.

Furthermore, the strain of graphene is related to its tension, and the tension is associated with the frequency shift of the graphene 2D peak. Therefore, the strain of the graphene layer is given by:

$$\dot{o}_g = -\frac{\Delta\omega_{2D}}{\gamma_{2D}(1-\nu_g)\omega_{2D}^0} \tag{4}$$

where γ_{2D} is the Grüneisen parameter, with a value of 1.99. ν_g is the Poisson's ratio of graphene. ω_{2D}^0 is the 2D-peak position under zero-strain condition. $\Delta\omega_{2D}$ is the shift of the 2D-peak relative to the zero-strain state.

Combining Equations (1), (2), (3), and (4), the fundamental frequency of the

Graphene/Parylene-C composite membrane is given by:

$$f_{01} = \frac{2.405}{2\pi a}\sqrt{\frac{-\frac{\Lambda\omega_{2D}}{\gamma_{2D}(1-\nu_g)\omega_{2D}^0}(E_P h_P + N h_{SLG} E_g)}{h_P\rho_P + N h_{SLG}\rho_g}} \tag{5}$$

2.2 Finite-Element Simulation of CMUT Cells

A three-dimensional finite-element model of a CMUT cell is developed in COMSOL Multiphysics 6.3 (COMSOL Inc.) using the Solid Mechanics, Electrostatics, and Membrane physics interfaces. The model comprises a substrate, a bottom electrode, an insulating layer, support walls, a cavity, and a composite membrane. The composite membrane is represented using the Membrane interface. A schematic of the model is shown in Figure 1, and the corresponding parameters are listed in Table 1.

Table 1 Main Parameters of CMUT Cells with Graphene/Parylene-C Composite Membrane

parameters	Value	Description
h_c	2μm	Cavity height
a	30μm	Membrane radius, Cavity radius
h_P	0.1μm	Parylene-C layer thickness
E_P	3.2GPa	Young's modulus of the Parylene-C layer
ρ_P	1289kg/m^3	Density of the Parylene-C layer
h_{SLG}	0.34nm	Thickness of single-layer graphene
N	2	Number of graphene layers
E_g	1050GPa	Young's modulus of graphene
ρ_g	2270 kg/m^3	Density of graphene
ν_g	0.199	Poisson's ratio of graphene

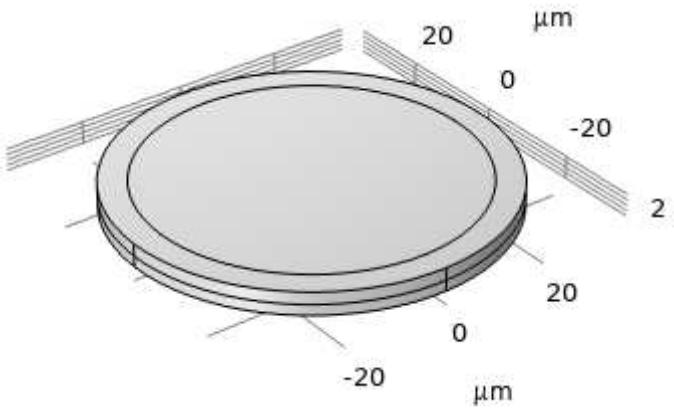


Fig.1 Schematic Diagram of the Three-Dimensional Model of CMUT Cell

During CMUT operation, a DC bias voltage is applied to establish a statically deflected membrane state, thereby enhancing acoustic output and receive sensitivity. The bias voltage is typically set to approximately 80% of the collapse voltage. A lower collapse voltage enables operation at a reduced bias voltage, potentially simplifying the drive circuitry and reducing its power requirements while maintaining effective electromechanical coupling. Therefore, the effects of structural parameters on the CMUT collapse voltage are investigated first.

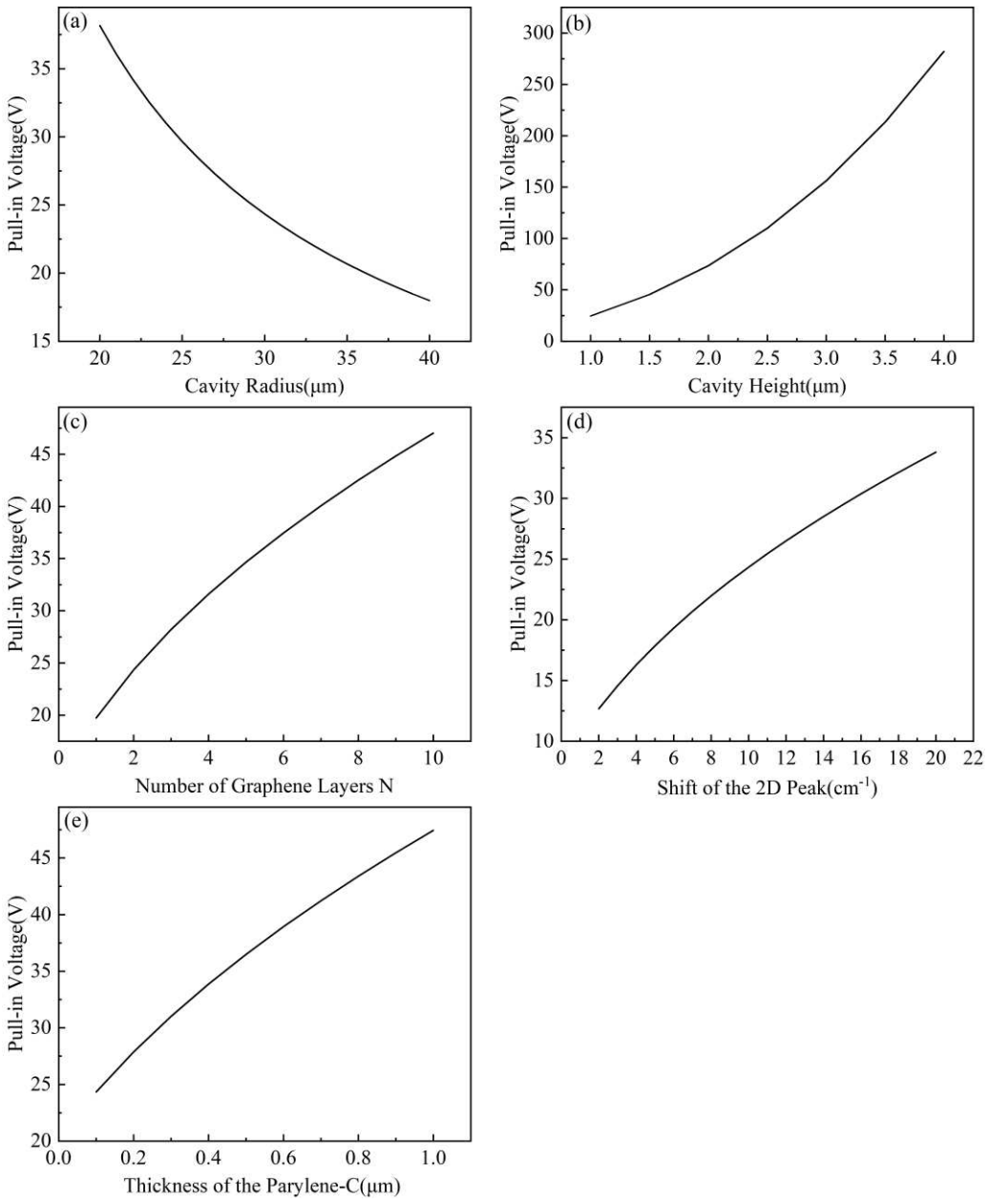


Fig.2 Relationships between CMUT collapse voltage and various structural parameters: (a) Cavity radius; (b) Cavity height; (c) Number of graphene layers; (d) 2D-peak frequency shift in wavenumber; (e) Parylene-C thickness

As shown in Figure 2, collapse in the graphene/Parylene-C composite-membrane CMUT occurs when the electrostatic attraction exceeds the membrane's restoring force, resulting in mechanical instability. The cavity dimensions determine the electrostatic loading and the membrane area over which it acts, while the composite membrane's in-plane tensile stiffness and residual tensile stress jointly govern its resistance to transverse deformation. Increasing the cavity radius enlarges the loaded membrane area and lowers the collapse voltage, whereas increasing the cavity gap reduces the electrostatic attraction at a given voltage and raises the collapse voltage. Increasing either the number of graphene layers or the Parylene-C thickness enhances the effective in-plane tensile stiffness of the composite membrane. Furthermore, adjusting the initial in-plane tensile stress,

as reflected by the shift in graphene's 2D Raman peak, provides a means of tuning membrane pretension without changing its geometry. Higher pretension improves resistance to collapse and increases the collapse voltage.

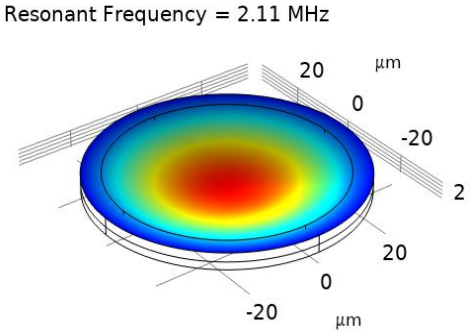


Fig.3 Schematic of the first-order characteristic frequency

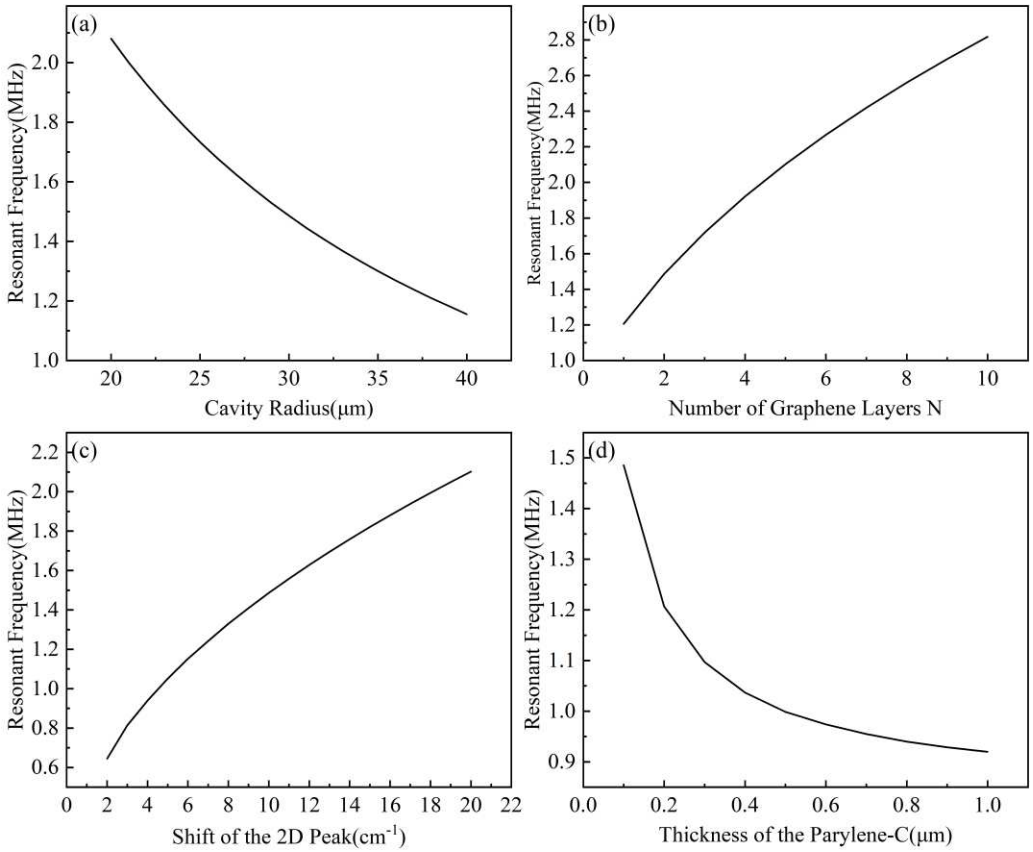


Fig.4 Relationships between CMUT characteristic frequency and various structural parameters: (a) Cavity radius; (b) Number of graphene layers Parylene-C thickness; (c) 2D-peak frequency shift in wavenumber; (d) Number of graphene layers

As shown in Figure 3, the fundamental mode is characterized by in-phase membrane motion, with the maximum vibration amplitude at the membrane center. This mode promotes efficient acoustic radiation and electromechanical conversion, making it suitable for ultrasonic transmission and reception. Accordingly, its resonant frequency is selected as the characteristic frequency of the CMUT cell in this study. As shown in Figure 4(a)–(d), the characteristic frequency of the graphene/Parylene-C composite-membrane CMUT decreases with increasing cavity radius and

Parylene-C thickness, but increases with the number of graphene layers and the wavenumber shift of graphene's 2D Raman peak. These trends are consistent with Equation (5).

Overall, the structural parameters jointly influence the collapse voltage and characteristic frequency, requiring a balance between stable operation under electrical bias and the desired acoustic operating frequency. Based on the optimization results, the selected design comprises a cavity radius of 30 μm, a cavity height of 1 μm, two graphene layers, and a Parylene-C thickness of 0.1 μm. This configuration yields a collapse voltage of 24 V and a characteristic frequency of 1.48 MHz.

2.3 Simulation of Linear Phased Array

Based on the previous cell-level simulation results, CMUT cells featuring low-voltage driving and high-frequency performance are achieved. Nevertheless, array-level simulation is essential to evaluate its performance under practical application scenarios. Accordingly, an in-depth analysis is carried out in the following section.

A two-dimensional model is developed in COMSOL using the Pressure Acoustics, Frequency Domain interface to investigate the focusing performance of the graphene/Parylene-C composite-membrane linear phased array. As shown in Figure 5, the model comprises a rectangular acoustic propagation domain with the linear array positioned along its lower boundary. The array element pitch is set to 0.54 mm, approximately half the acoustic wavelength. This spacing satisfies the spatial Nyquist sampling criterion and helps suppress grating lobes, thereby improving imaging.

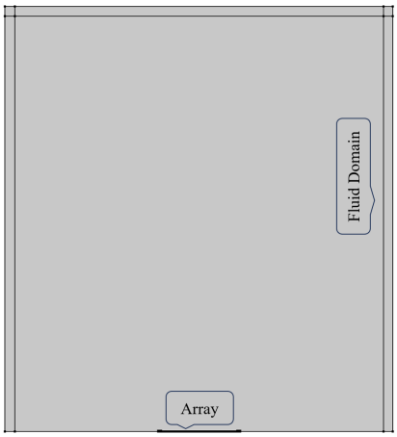


Fig.5 Schematic of the Simulation Model

The working medium consists of general human soft tissue, with a density of 1040 kg/m³ and a sound speed of 1540 m/s. The material attenuation law is given by the following expression:

$$\alpha(f) = \alpha_{ref}\left(\frac{f}{f_{ref}}\right)^{n} \tag{6}$$

where the attenuation constant at the reference frequency f_{ref} =1MHz is α_{ref} =5.57Np/m, and n = 1.2.

The element width is constrained by the array pitch and therefore cannot be selected independently. Increasing the element width raises the fill factor, resulting in higher focal acoustic pressure and improved sidelobe suppression. As shown in Figure 6, increasing the element width from 0.2λ to 0.4λ gradually increases the focal acoustic pressure and decreases the full width at half maximum (FWHM), indicating improved lateral resolution. Thus, increasing the element width

within the constraints imposed by the array pitch can enhance focusing performance.

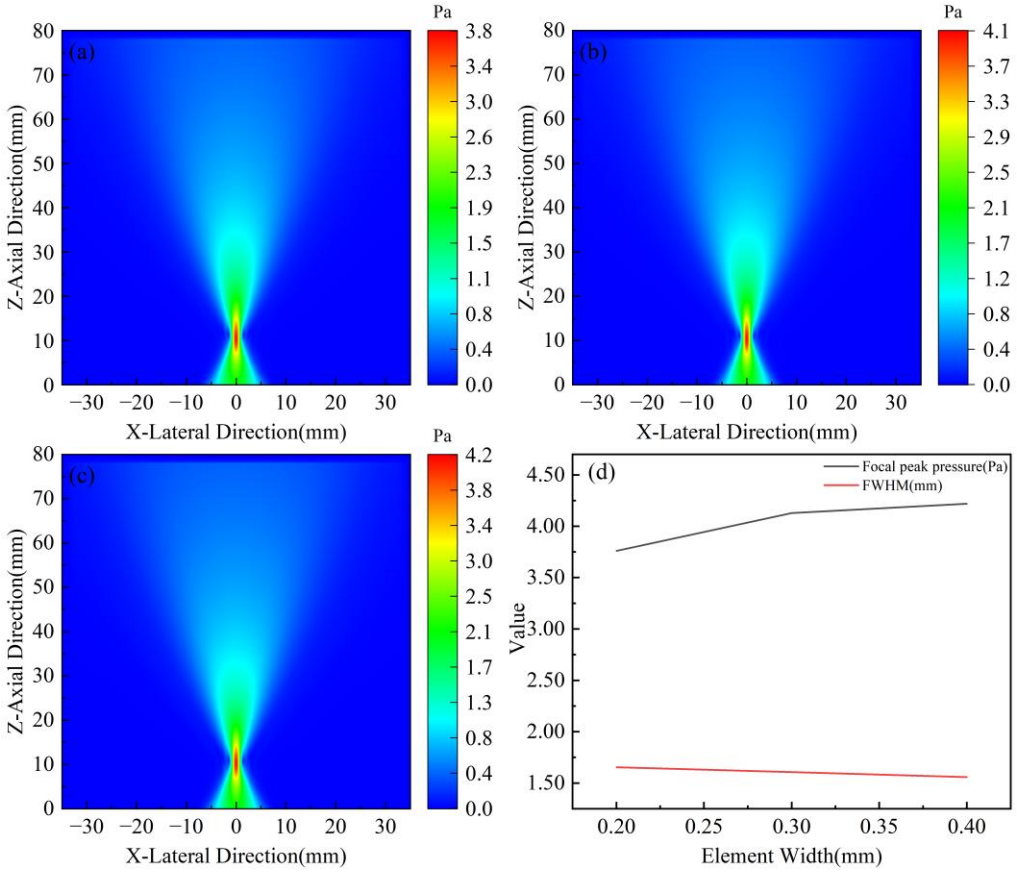


Fig.6 Simulation results under different element widths: (a) 0.2λ; (b)0.3λ ; (c)0.4λ ; (d) Variations of sound pressure value and FWHM at the focal point

The number of active elements N directly determines the beam profile and focusing intensity. In this work, analyses are carried out for $N = 8$, 16, and 32.

As shown in Figure 7(a)-(c), the sound-pressure value at the focal point gradually increases with the rising number of active elements N. To further evaluate the lateral resolution performance, the transverse beam-profile curve at the focal point is extracted, as presented in Figure 7(d), and its full width at half-maximum (FWHM) is calculated. The results demonstrate that for $N = 8$, 16 and 32, the corresponding FWHM values are 5.57 mm, 3.11 mm and 2.10 mm, showing a distinct decreasing trend. This indicates that increasing the number of elements effectively improves the lateral resolution of the phased array. Considering both performance gain and implementation complexity, $N = 32$ is selected as the preferred configuration in this work.

Table 2 Acoustic Characteristic Parameters

	Z_f (focal length,mm)	L_{pmax} (sound pressure at Z_f,Pa)	FWHM (mm)	SLL (sidelobe level,dB)	DOF (depth of field,mm)
1MHz	30	2.92	5.56	-33.02	5.64
2.5 MHz	30	2.44	3.63	-33.85	5.19
5 MHz	30	0.87	4.64	-14.37	3.52
10 MHz	30	0.29	7.01	-12.46	4.18

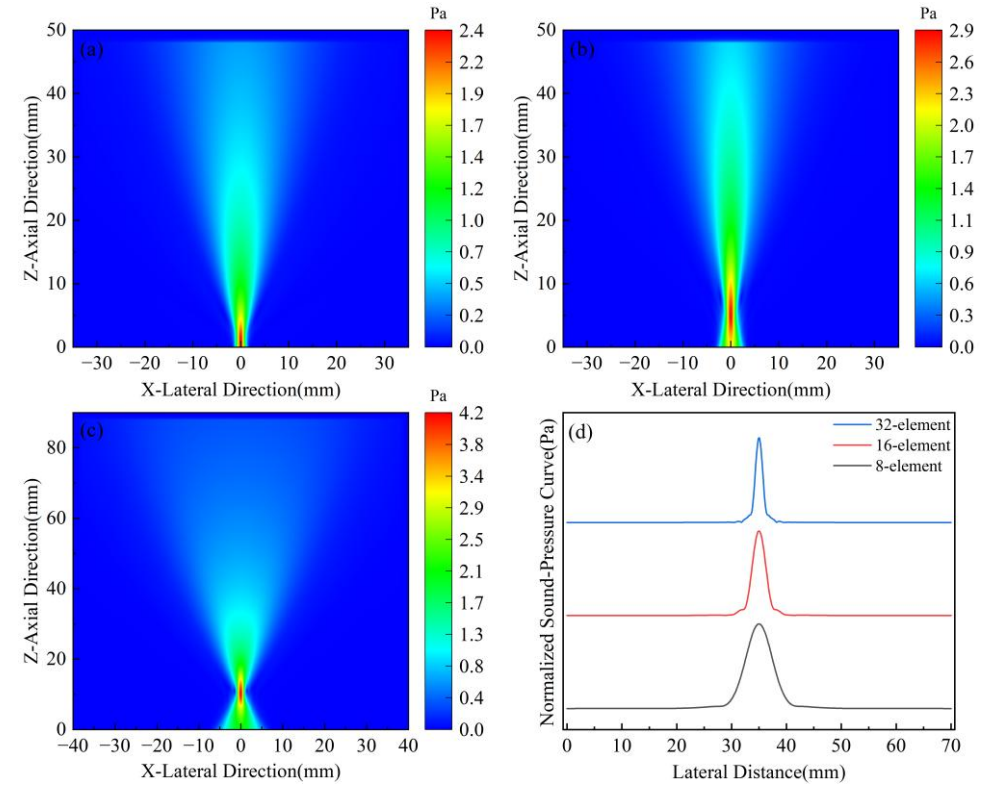


Fig.7 Simulation results for different numbers of array elements: (a) $N = 8$; (b) $N = 16$; (c) $N = 32$; (d) Transverse beam-profile curve at the focal point

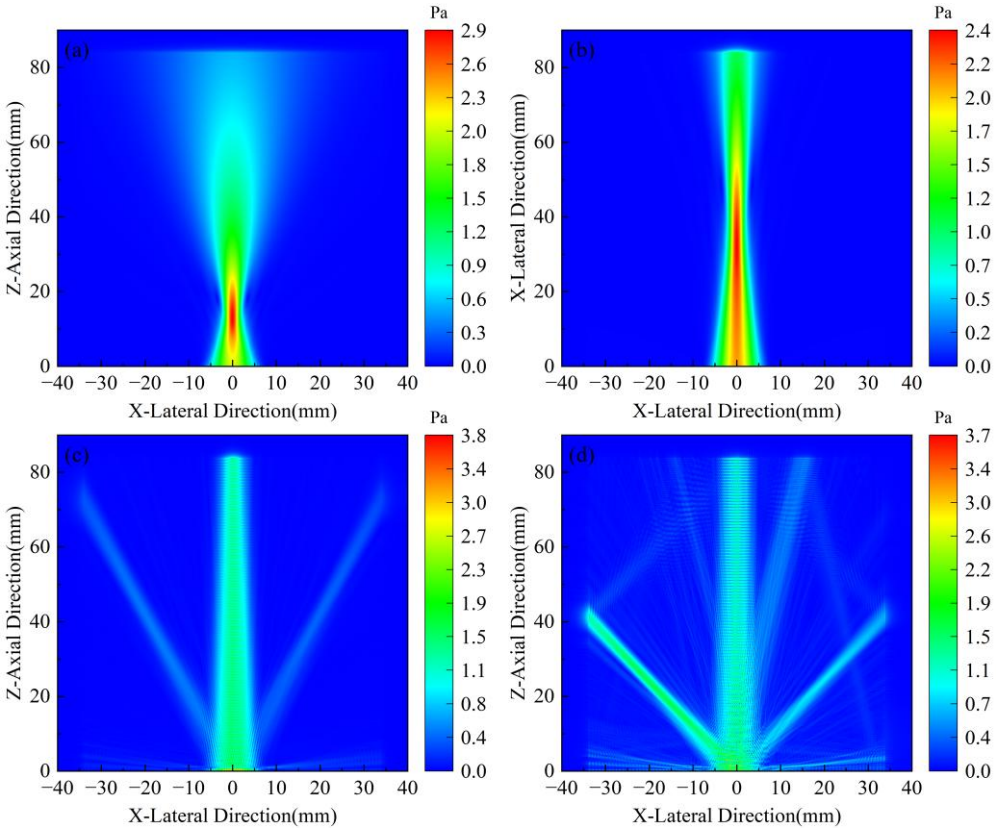


Fig.8 Sweep-frequency analysis of the linear phased array: (a) 1 MHz; (b) 2.5 MHz; (c) 5 MHz; (d) 10 MHz

Sweep-frequency simulations from 1 MHz to 10 MHz are carried out for the linear ultrasonic phased array. The results are presented in Figure 8 and Table 2. Within the low-frequency range (1 MHz, 2.5 MHz), favorable beam-focusing performance is achieved. As the frequency increases moderately, the FWHM of the focused beam decreases and the lateral resolution is improved. In the mid-to-high frequency range (5 MHz-10 MHz), ultrasonic waves suffer much stronger attenuation inside the medium, which leads to a remarkable drop in sound pressure at the focal point. The variations in FWHM and SLL (sidelobe level) indicate beam broadening, degraded lateral resolution and severe sidelobe interference. In summary, the proposed phased-array design is more suitable for operation in the low-frequency regime.

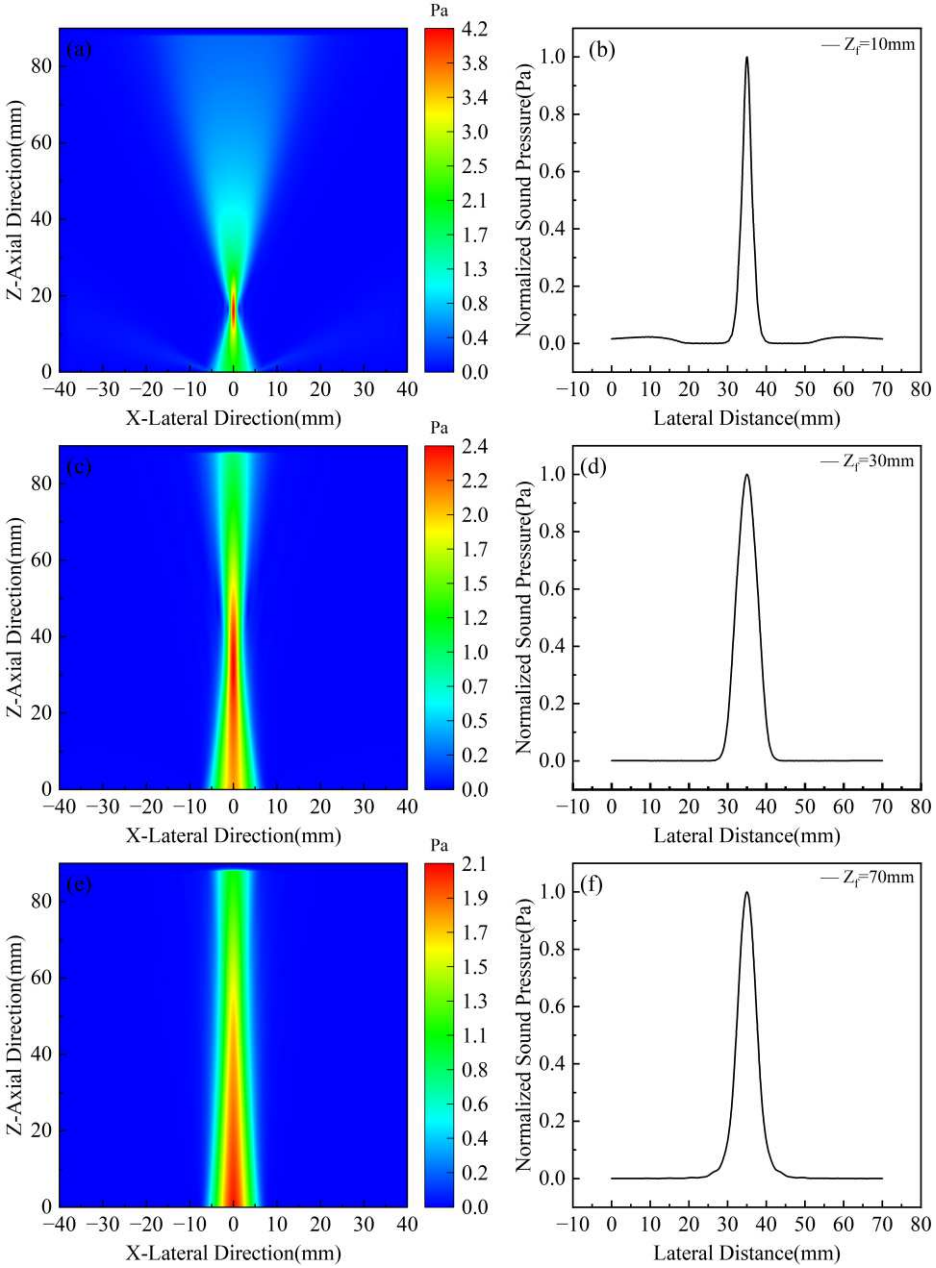


Fig.9 Contour plots of focal-plane sound-pressure distribution under different focal lengths: (a) 10 mm; (c) 30 mm; (e) 70 mm; Normalized transverse sound-pressure distribution curves at the focal point: (b) 10 mm; (d) 30 mm; (f) 70 mm

Variable-focal-length simulations (Figure 9) show that at a fixed frequency of 2 MHz, increasing the focal length from 10 mm to 30 mm leads to an increase in FWHM and a slight degradation of lateral resolution, while the depth of field is enhanced and the effective imaging range is broadened. Nevertheless, an excessively large focal length (70 mm) causes sharp divergence of FWHM accompanied by acoustic-pressure attenuation, which degrades the overall focusing performance. Therefore, for the present array configuration, a reasonable trade-off between lateral resolution and detection depth should be made according to practical application scenarios.

3 Conclusion

This study proposes a CMUT cell incorporating a graphene/Parylene-C composite membrane, combining the electrical and mechanical properties of graphene with the flexibility and biocompatibility of Parylene-C. A finite-element model coupling electrostatic, structural, and acoustic physics is developed in COMSOL Multiphysics to optimize the cell design and evaluate the acoustic performance of a one-dimensional phased array. The main conclusions are as follows:

(1) Parametric sweeps reveal the effects of cavity radius, cavity height, Parylene-C thickness, graphene layer number, and graphene's 2D Raman peak shift, which reflects membrane prestress, on the collapse voltage and characteristic resonant frequency. The optimized cell has a cavity radius of 30 μm, a cavity height of 1 μm, two graphene layers, and a Parylene-C thickness of 0.1 μm. This configuration yields a collapse voltage of 24 V and a characteristic frequency of 1.48 MHz, balancing a relatively low bias voltage with the desired operating frequency.

(2)A one-dimensional linear phased-array model is constructed using the optimized cell design. The effects of element width, active element number, and focal length on beam focusing, focal acoustic pressure, and lateral resolution are evaluated. The simulation results demonstrate the array's focusing capability and support its potential for ultrasonic imaging.

By combining complementary membrane materials with coupled multiphysics simulations, this study provides a foundation for the design and optimization of flexible MEMS ultrasonic transducers.

Acknowledgments

This work was partially sponsored by Southwest Jiaotong University's "Cao Jianyou" development funds (No. JZ0111041605) and the Fundamental Research Funds for the Central Universities (2682025CX134).

References

Oluwafemi J. Adelegan, Zachary A. Coutant, Xiao Zhang, Feysel Yalcin Yamaner ,Omer Oralkan (2020). "Fabrication of 2D Capacitive Micromachined Ultrasonic Transducer (CMUT) Arrays on Insulating Substrates With Through-Wafer Interconnects Using Sacrificial Release Process." Journal of Microelectromechanical Systems 29(4): 553–561. http://dx.doi.org/10.1109/jmems.2020.2990069

Anouar Boujenoui, Nadia El Atlas, Abdelmajid Bybi, Hayat Reskal ,Lahoucine Elmaimouni (2025). "Advances in Crosstalk Reduction Techniques for Ultrasonic Transducer Arrays." Sensors 25(24). http://dx.doi.org/10.3390/s25247666

Morris Ming-Wei Chang, Milton T-M. Deng, James T-J. Gwo, John D. Mai, Elmer Hsu ,Ieee (2006). Polymer-based capacitive micromachined ultrasonic transducers (CMUT) for micro surgical

Imaging applications. IEEE International Conference of Nano/Micro Engineered and Molecular Systems, Zhuhai, PEOPLES R CHINA.

Po-Fat Chong, Xiaomei Shi ,Ching-Hsiang Cheng (2014). "Capacitive micromachined ultrasonic transducer (CMUT) array with single-layer graphene membrane." Micro & Nano Letters 9(12): 884–886. http://dx.doi.org/10.1049/mnl.2014.0421

Po-Fat Chong, Xiaomei Shi, Ching-Hsiang Cheng ,Ieee (2013). A Novel Flexible Capacitive Micromachined Ultrasonic Transducer (CMUT) Array With Isolated Metallic Islands Riveted To A Polymer Film. 8th Annual IEEE International Conference on Nano/Micro Engineered and Molecular Systems (NEMS), Suzhou, PEOPLES R CHINA.

Rongrong Guo, Guolan Lu, Binjie Qin ,Baowei Fei (2018). "ULTRASOUND IMAGING TECHNOLOGIES FOR BREAST CANCER DETECTION AND MANAGEMENT: A REVIEW." Ultrasound in Medicine and Biology 44(1): 37–70. http://dx.doi.org/10.1016/j.ultrasmedbio.2017.09.012

Changde He, Binzhen Zhang, Chenyang Xue, Wendong Zhang ,Shengdong Zhang (2021). "Wafer-Bonding Fabricated CMUT Device with Parylene Coating." Micromachines 12(5). http://dx.doi.org/10.3390/mi12050516

Carl D. Herickhoff ,Rob Van Schaijk (2023). "cMUT technology developments." Zeitschrift Fur Medizinische Physik 33(3): 256–266. http://dx.doi.org/10.1016/j.zemedi.2023.04.010

Llkhechi Afshin Kashani, Maadi Mohammad, Haven Nathaniel J M ,Zemp Roger J (2022). "Outperforming piezoelectric ultrasonics with high-reliability single-membrane CMUT array elements." Microsystems & Nanoengineering 8(3).

Maria Kim, Ali Shah, Changfeng Li, Petri Mustonen, Jannatul Susoma, Farshid Manoocheri, Juha Riikonen ,Harri Lipsanen (2017). "Direct transfer of wafer-scale graphene films." 2D Materials 4(3): 035004.

Makiko Kobayashi, Cheng-Kuei Jen ,Daniel Levesque (2006). "Flexible ultrasonic transducers." IEEE transactions on ultrasonics, ferroelectrics, and frequency control 53(8): 1478–1486.

Jiapu Li, Yuqing Ma, Tao Zhang, K. Kirk Shung ,Benpeng Zhu (2022). "Recent Advancements in Ultrasound Transducer: From Material Strategies to Biomedical Applications." BME frontiers 2022. http://dx.doi.org/10.34133/2022/9764501

Jie Liu, Haodong Chen, Youming Luo ,Quanfang Chen (2024). "Analytical and experimental study on bilayer membrane-type Capacitive Micromechanical Ultrasonic Transducer." Sensors and Actuators a-Physical 376. http://dx.doi.org/10.1016/j.sna.2024.115639

Jie Liu, Yuyao Li, Youming Luo ,Quanfang Chen (2023). "Capacitive Micromachined Ultrasonic Transducer (CMUT) Made with SWCNTs/Parylene-C Composite Membranes." Acs Applied Electronic Materials 5(8): 4316–4322. http://dx.doi.org/10.1021/acsaelm.3c00585

Jun Ma, Wei Jin, Hoi Lut Ho ,Ji Yan Dai (2012). "High-sensitivity fiber-tip pressure sensor with graphene diaphragm." Optics Letters 37(13): 2493–2495. http://dx.doi.org/10.1364/ol.37.002493

Mohammad Mahdi Tavakoli, Giovanni Azzellino, Marek Hempel, Ang-Yu Lu, Francisco J. Martin-Martinez, Jiayuan Zhao, Jingjie Yeo, Tomas Palacios, Markus J. Buehler ,Jing Kong (2020). "Synergistic Roll-to-Roll Transfer and Doping of CVD-Graphene Using Parylene for Ambient-Stable and Ultra-Lightweight Photovoltaics." Advanced Functional Materials 30(31). http://dx.doi.org/10.1002/adfm.202001924

Zhen Wan, Cheng Li, Zhengwei Wu, Pengcheng Zhao, Yang Liu, Wanting Li, Shangchun Fan ,Wei Jin

(2026). "Ultra-Sensitive Dual-Resonator Graphene Pressure Sensor with Temperature Self-Compensation." Advanced Science 13(5). http://dx.doi.org/10.1002/advs.202517536

Haosheng Xu, Shaohui Yang, Qi Lai, Xuemei Gao, Weijuan Chen ,Xiaojing He (2025). "Active time-reversal based phased array ultrasound system for accurate focusing through biological tissue layers." Discover Nano 20(1). http://dx.doi.org/10.1186/s11671-025-04331-6

Yuanyu Yu, Xin Liu, Jiujiang Wang ,Shuang Zhang (2026). "Advances and Challenges of Capacitive Micromachined Ultrasonic Transducers in Medical Imaging." Micromachines 17(4). http://dx.doi.org/10.3390/mi17040486